Complex dynamics in polymer nanocomposites

S. Srivastava,[1] A. K. Kandar,[1] J. K. Basu,[1,*] M. K. Mukhopadhyay,[2] L. B. Lurio,[3] S. Narayanan,[4] and S. K. Sinha[2]
[1]*Department of Physics, Indian Institute of Science, Bangalore, 560 012, India*
[2]*Department of Physics, University of California San Diego, La Jolla, California 92093, USA*
[3]*Department of Physics, Northern Illinois University, De Kalb, Illinois 60115, USA*
[4]*Advanced Photon Source, Argonne National Laboratory, Argonne, Illinois 60439, USA*
(Received 15 November 2008; published 25 February 2009)

Polymer nanocomposites offer the potential to create a new type of hybrid material with unique thermal, optical, or electrical properties. Understanding their structure, phase behavior, and dynamics is crucial for realizing such potentials. In this work we provide an experimental insight into the dynamics of such composites in terms of the temperature, wave vector, and volume fraction of nanoparticles, using multispeckle synchrotron x-ray photon correlation spectroscopy measurements on gold nanoparticles embedded in polymethylmethacrylate. Detailed analysis of the intermediate scattering functions reveals possible existence of an intrinsic length scale for dynamic heterogeneity in polymer nanocomposites similar to that seen in other soft materials like colloidal gels and glasses.

DOI: 10.1103/PhysRevE.79.021408 PACS number(s): 82.70.−y, 64.70.qj, 61.05.cf, 64.70.km

I. INTRODUCTION

Polymer nanocomposites (PNC) are a class of multifunctional hybrid materials which are obtained by appropriate mixing of nanoparticles and polymers leading to a wide range of applications in terms of their unique electrical, optical, and thermomechanical properties [1–4]. They also belong to this class of materials, under the umbrella of soft glassy materials, which exhibit rich and complex thermal, mechanical and rheological behavior [5–11]. Extensive experimental work has been performed over the decade or so on studying the modifications of thermal and mechanical properties imparted to the matrix polymer by addition of nanoparticles of various shapes and sizes [4,12–15]. Numerical simulations and theoretical calculations have started to emerge in the meanwhile to provide some insight and understanding into the static structure and phase behavior in various model nanoparticle-polymer hybrid systems [16–20]. Homogeneous dispersion of nanoparticles in polymer matrices is a major obstacle [3] towards the ultimate goal of obtaining high performance materials. In this respect it has been observed by us [4] and a few other groups [21] that using a polymer capped nanoparticle in a matrix of chemically matched homopolymer matrix is a very effective way of ensuring homogeneous dispersion. However, the theory and simulations for the static structure and phase behavior for such systems are only just beginning to emerge [16–20] and a microscopic theory to treat the dynamics, of both polymer capped and uncapped nanoparticles in polymer matrices, including viscoelasticity, glass formation or diffusion of nanoparticles does not exist. Dynamics of soft glassy materials is extremely rich and complex [5,7,22–24]. Depending on various parameters like volume fraction, (ϕ) and temperature, (T) such systems exhibit complex slow dynamics characteristic, of glassy or jammed phase [5,7,22–24]. Dynamic heterogeneity is a key feature of such systems and evidence of length scale dependent dynamic heterogeneity has been observed in simulations [10,25,26] and certain experiments [27,28]. Here we provide evidence for possible existence of a length scale of dynamic heterogeneity for PNC. We also provide a glimpse of the complexity and richness of dynamics of polymer nanocomposites as a function of ϕ, T, and the wave vector, q, through detailed synchrotron multispeckle x-ray photon correlation spectroscopy (XPCS) measurements.

In Sec. II we discuss in detail the synthesis method for polymethylmethacrylate (PMMA) capped gold nanoparticles dispersed in PMMA matrix, their characterization using transmission electron microscopy (TEM) and estimation of glass transition temperature (T_g) using modulated differential scanning caloriemetry (MDSC). We also describe the basics of XPCS technique followed by the experimental details for the measurement of our sample. Section III describes the details of the experimental observation including systematic variation of the intensity autocorrelation functions as a function of measured temperature, volume fraction, and wave vector, as extracted from XPCS measurements. We extract the relaxation time, τ, and the Kohlrausch exponent, β, from the correlation functions to provide insight into the complex nature of dynamics in the PNC systems studied here and provide a perspective on how this compares with behavior observed in other related soft matter systems. Finally in Sec. IV we provide our conclusions and outlook on the measured dynamics.

II. EXPERIMENTAL METHODS

A. Sample preparation

All chemicals, hydrogen tetrachloroauric acid ($HAuCl_4$), PMMA (molecular weight 120 K), sodium borohydride ($NaBH_4$), were obtained from Sigma-Aldrich chemicals and were used without any treatment. Ethanol was obtained from Merck. Deionized water (18.2 mΩ, Barnstead) was used for all experiments. The gold nanoparticles capped with PMMA

*basu@physics.iisc.ernet.in

and embedded in the same PMMA matrix, were prepared by reduction of $HAuCl_4$ with $NaBH_4$ in the presence of PMMA [4]. The particles of different sizes were obtained by changing the concentration of the capping polymer. Samples for measurements in the powder form were made by controlled evaporation of the nanocomposite solution at 70 °C in either a good (acetone) or a bad solvent (acetone: water, 1:10) [4]. Powder samples were annealed at 150 °C for 24–30 h under a vacuum of 5×10^{-4} mbar for XPCS measurements.

B. Sample characterization

The size of the PMMA-capped nanoparticles were quantitatively estimated from TEM (Technai F-30) images as shown in Fig. 1 using an operating voltage of 300 KV. The samples for measurements were prepared by drop casting nanoparticle solution on a carbon-coated grid followed by drying for 4–5 h. The quantitative estimate of size and polydispersity was obtained by plotting a histogram over ~200 particles taken over different regions. As is clear from the TEM images, the nanoparticles are uniformly dispersed in the PMMA matrix. The particles of larger size are obtained by reducing the concentration of the capping polymer. Larger polymer concentration gives relatively more monodisperse nanoparticles. The results presented here, are based on three different samples (A,B,C), of nanocomposite consisting of gold nanoparticles of mean diameter, 4.0 ± 0.7 nm, 5.0 ± 1.3 nm, and 10.0 ± 2.0 nm, respectively, embedded in PMMA matrix. The calculated volume fraction ϕ of gold in the above-mentioned samples are 0.006, 0.012, and 0.077, respectively. The thermal behavior of the samples were analyzed by using MDSC (TA Instrument (2920CE). The MDSC measurements were performed using an instrument equipped with liquid nitrogen cooling accessory. Several thermal cycles were performed to remove the thermal history. Initial heating up to 150 °C followed by cooling down to 50 °C; heating at a constant underlying rate of 3 °C/min up to 150 °C; cooling at the same rate down to 50 °C; reheating at the same rate up to 150 °C with modulation period of 100 s and amplitude of ±1 °C followed by modulated cooling down to 50 °C. The T_g estimates were made from complex heat capacity data, heat flow phase, and the reversible heat flow. Here we have presented the complex heat capacity data to estimate respective T_g for samples A, B, C and as well as for neat PMMA. The glass transition temperature estimated from the complex heat capacity signal were found to be 392 K for sample A, 380 K for sample B, and 381 K for sample C. The T_g for neat PMMA were estimated to be 390 K as shown in Fig. 2.

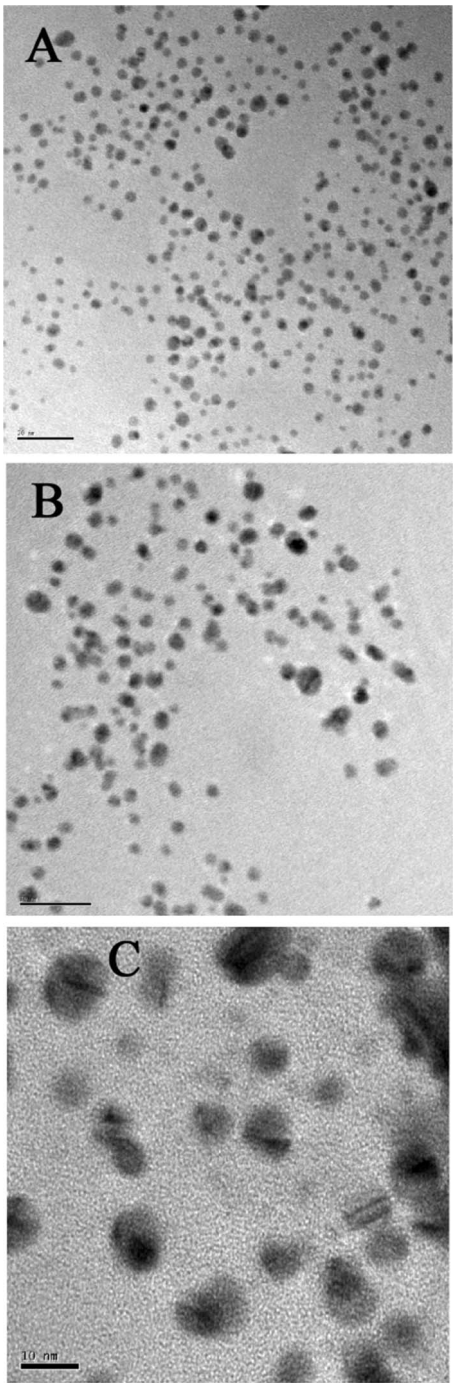

FIG. 1. The TEM images for samples A, B, and C containing gold nanoparticles of mean diameter 4.0 ± 0.7 nm, 5.0 ± 1.3 nm, and 10.0 ± 2.0 nm, respectively, dispersed homogeneously in PMMA matrix.

C. X-ray photon correlation spectroscopy

In XPCS one measures the intensity autocorrelation function [9,11,14,29],

$$g_2(q,t) = 1 + b|f(q,t)|^2. \quad (1)$$

Here, $f(q,t)$ is the intermediate scattering function (ISF), b is the speckle contrast, and t is the delay time. We have used ISF of the general form

$$f(q,t) = \exp[-(t/\tau)^{\beta}], \quad (2)$$

where τ and β represents the characteristic relaxation time of the system and the Kohlrausch exponent, respectively. The mean relaxation time, τ follows a power-law behavior and is given by

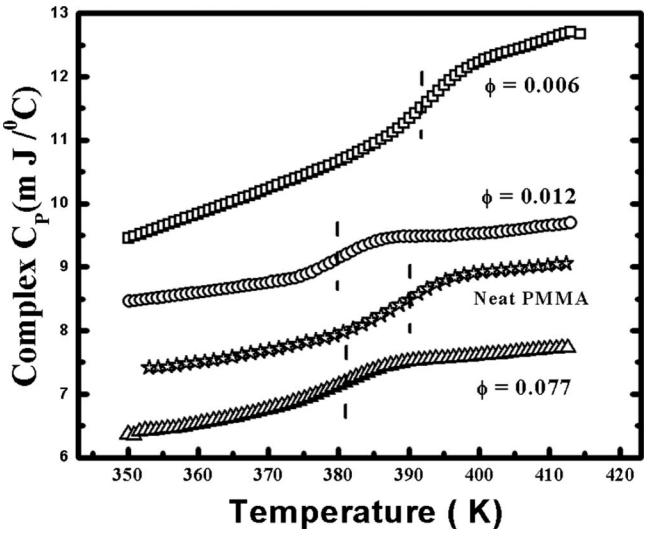

FIG. 2. MDSC data for samples A, B, and C. The dashed lines drawn at the midpoint of the transition region for the respective data indicate the glass transition temperature T_g for samples A (□), B (○), C (△), and neat PMMA (★), respectively (refer to the text). Indicated alongside each curve are the respective volume fractions, ϕ of gold in the PMMA matrix.

$$\tau \propto q^{-\alpha}. \tag{3}$$

For diffusive motion, $\alpha=2$. However, for ballistic or superdiffusive motion α is predicted to be ~ 1 and for subdiffusive motion $\alpha > 2$ [30]. Normally, β is independent of q, however there has been some recent observation in colloidal gel systems where β has also been found to depend on q [27,28]. However, the underlying physics is not clear. We performed XPCS measurements at 8-ID, beamline of the Advance Photon Source with partially coherent x rays of energy 7.35 KeV of beam size 20 μm $\times$ 20 μm using a CCD (Princeton Instruments). The total exposure time at each sample position was limited to $\sim$10 minutes to minimize radiation damage.

III. RESULTS AND DISCUSSIONS

Since x-rays are mostly sensitive to the scattering contrast between gold nanoparticle and PMMA, the observed dynamics is mostly a reflection of the motion of the PMMA capped gold nanoparticles through the background of matrix PMMA and is essentially sensitive to the length scale dependent viscoelastic property of the medium. However, the motion of these polymer capped particles could be different from that of uncoated nanoparticles in gels [9] or supercooled liquids [11], since apart from volume fraction the interface morphology at the polymer particle interface as well as grafted chain-free matrix chain interaction could decide the over all dynamics as well. We have shown earlier how the interface morphology affects the T_g of the PNC at fixed volume fraction and is not very sensitive to core size [4]. Hence we believe that although the PNC dynamics should essentially be a reflection of the gold nanoparticle motion in PMMA matrix it (dynamics) might not be as simple as colloidal sphere diffusion in a homogeneous medium. With this perspective let us discuss the interesting dynamics observed in our PNC samples as a function of temperature, T, volume fraction, ϕ and wave vector, q. For sample A ($\phi=0.006$) we find that the intensity autocorrelation function, $g_2(t)$, shows nonexponential decay depending on the measured temperature, T, or wave vector, q, as indicated in Fig. 3. Specifically, Fig. 3(b) shows that at low temperatures, the relaxation is stretched ($\beta<1$) while in Fig. 3(a) at the highest measured temperature, it is compressed ($\beta>1$). Similarly, for sample B ($\phi=0.012$) we find that $g_2(t)$ shows compressed exponential relaxation at high temperature [Fig. 4(a)] while at lower temperatures it shows stretched exponential relaxation [Fig. 4(b)]. Surprisingly, sample C ($\phi=0.077$) does not show stretched exponential relaxation at any measured temperature or wave vectors. However, it is found to show compressed exponential relaxation at low wave vector and high temperatures as indicated in Fig. 5. It is clear that the relaxations in the PNC samples evolves as a function of the various parameters ϕ, T, and q and shows stretched and/or compressed crossover as has been observed for some other soft matter samples [5,11,25]. However much better insight about complexity of the dynamics is obtained by looking at the dependence of β and τ, extracted using Eq. (2) and Eq. (3) in Eq. (1), on these parameters. In Fig. 6 we depict the variation of β and τ with q and T for the lowest volume fraction of PNC

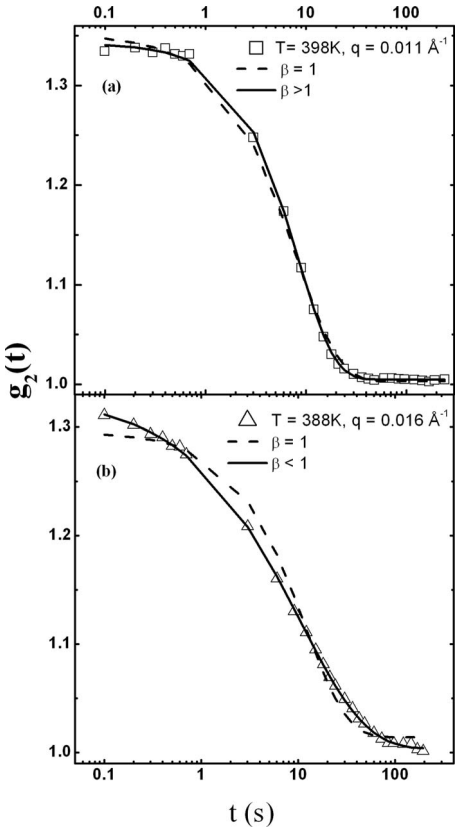

FIG. 3. $g_2(t)$ vs t, showing different types of relaxation behavior observed for sample A ($\phi=0.006$). (a) Compressed exponential relaxation and (b) stretched exponential relaxation. Dashed and solid lines are the exponential and nonexponential ($\beta \neq 1$) fits to the respective data in each panel. The temperature and q values for the corresponding data are indicated in each panel.

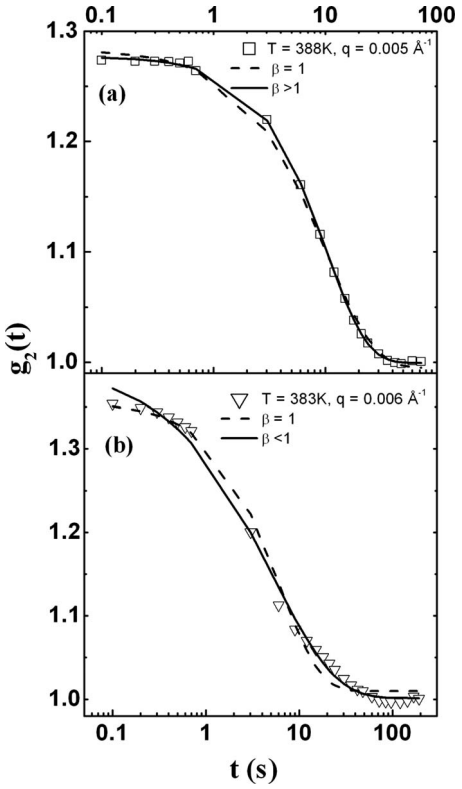

FIG. 4. $g_2(t)$ vs t, showing different types of relaxation behavior observed for sample B (ϕ=0.012). (a) Compressed exponential relaxation and (b) stretched exponential relaxation. Dashed and solid lines are the exponential and nonexponential ($\beta \neq 1$) fits to the respective data in each panel. The temperature and q values for the corresponding data are indicated in each panel.

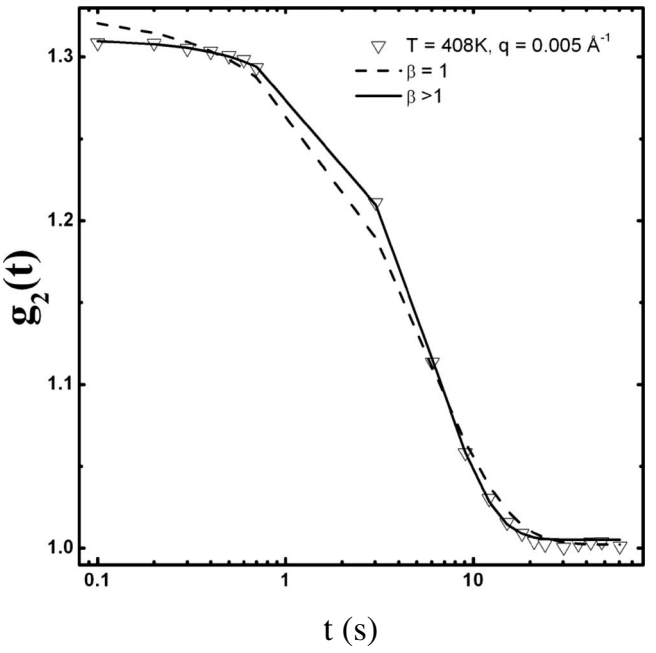

FIG. 5. $g_2(t)$ vs t, showing relaxation behavior observed for sample C (ϕ=0.077). Dashed and solid lines are the exponential and nonexponential ($\beta > 1$) fits to the data. The temperature and q values for the corresponding data are indicated in the panel.

sample. The striking crossover in β with temperature, as was also seen in the two ISF data in Fig. 3, is clearly visible. The ubiquitous $\beta > 1$ behavior which was observed earlier in various soft and granular materials undergoing jamming transition [5,7,10,11,22–24,27,28] as well as in a polymer nanocomposite [14], similar to ours, is also seen here and has been associated with the presence of anomalous diffusion. Although the data at $q > 0.03$ Å^{-1} is noisy it does seem to indicate that $\beta \to 1$ for all temperatures. At each temperature β seems to be almost independent of q over a large range. This temperature dependent crossover in β is opposite to what has been observed recently [11] and indicates fundamentally different dynamics as compared to nanoparticles in molecular supercooled fluids. The variation of τ with q is even more puzzling. At the lowest temperatures there clearly seems to be two values of α [Eq. (3)] in the low and high q regions, indicating length scale dependent dynamics. For example, at 383 K we get $\alpha(=\alpha_l)$ values of 0.39 ± 0.26 (standard deviation σ=1.7) at low q and $\alpha(=\alpha_h)$ is 0.75 ± 0.03 (σ=1.2) at high q. Using single straight line fit for the whole range of q we obtained $\alpha = 0.56 \pm 0.11$ (σ=2.2) clearly indicating that the two exponent (α) fit is much better. This is also true for the other temperatures as can be seen from the respective α values and the errors and standard deviations as indicated in each panel in Fig. 6. We find that in general α seems to increase with temperature in all q ranges. The exponent of $\alpha \sim 1$ and $\beta > 1$ has been associated with anomalous diffusion observed earlier in a similar PNC system [14] as well as in colloidal gels [22,24,27,28]. However to our knowledge dynamics with $\beta < 1$ and $\alpha \leqslant 1$ has not been observed earlier. The underlying physics is not clear. Interestingly, the q values at which the α crossover occurs seems to be independent of temperature and occurs at $q \sim 0.02$ Å^{-1} ($q = q_c$) and as indicated earlier, we will denote α_l as α for $q < q_c$ and α_h for $q > q_c$.

Turning our attention to the intermediate volume fraction (ϕ=0.012) sample we find approximately similar trends to that found for low volume fraction sample (sample A). As shown in Fig. 7(a), at the lowest measured temperatures (T =378 K and 383 K), we find that $\beta < 1$, indicating stretched relaxation while at high temperatures (T=388 K and 398 K) the relaxation is compressed, especially at the lower wave vectors. However, unlike the case of sample A we find here that within the error bars β has a dependence on q. The dependence of τ on q is quite intriguing. At all temperatures below 398 K, as shown in Figs. 7(b)–7(e), we find two values of α at low and high q with the respective values, their errors and standard deviation as indicated in the respective panels. Clearly a single α value does not fit the data well. Moreover, we find that both the α values generally tend to increase with increasing temperature while the q values at which the slope changes (q_c) is approximately 0.02 Å^{-1}. Even at the highest measured temperature for this volume fraction sample we find the existence of two α values although the effect seems to become weaker. As the volume fraction increases (ϕ=0.077) we find from Fig. 8(a) that the relaxations are predominantly compressed, especially at low q. It is interesting to note that although the measured T_g is almost the same for both samples B and C the relaxations are

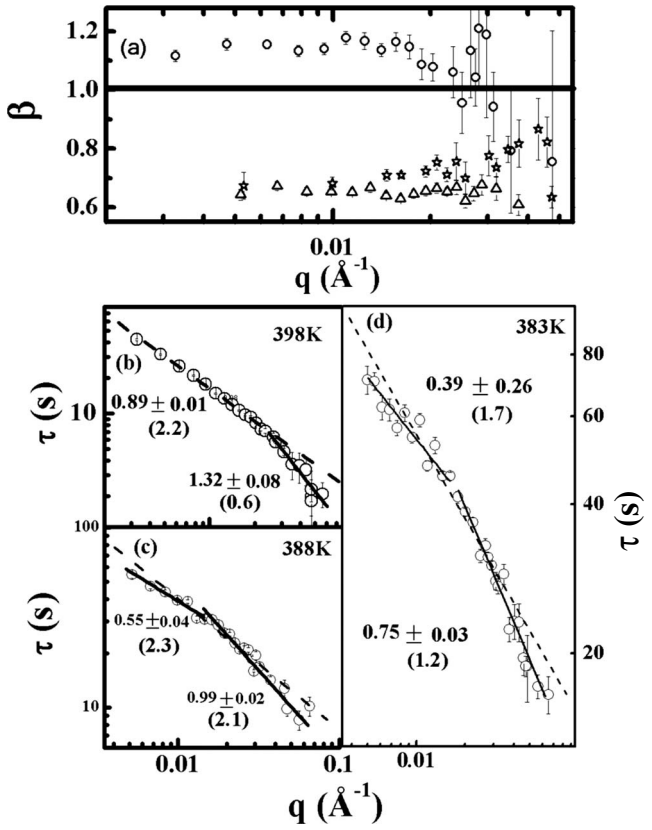

FIG. 6. (a) β vs q for PNC sample with ϕ=0.006 at different measured temperatures (T), ○, 398 K; △, 388 K; ★, 383 K. Relaxation time, τ vs q at various measured temperatures. (b) T =398 K, (c) T=388 K, and (d) T=383 K. The values of β and τ were extracted from fit to the $g_2(t)$ data using Eq. (2) and Eq. (3) in Eq. (1). Solid lines are the linear fits to the respective data in low and high wave-vector regions. Dashed lines are the fits to the same data over the entire measured range of wave vector. Indicated alongside each fitted curve is the estimate of respective α (α_l, α_h) obtained from the analysis using Eq. (3). The numbers within parentheses are the estimates of standard deviation for the obtained fits. The α value for the fit over the whole q range at 398 K, 388 K, and 383 K is 0.91 ± 0.01 (1.9), 0.73 ± 0.01 (3.14), and 0.56 ± 0.11 (2.2), respectively.

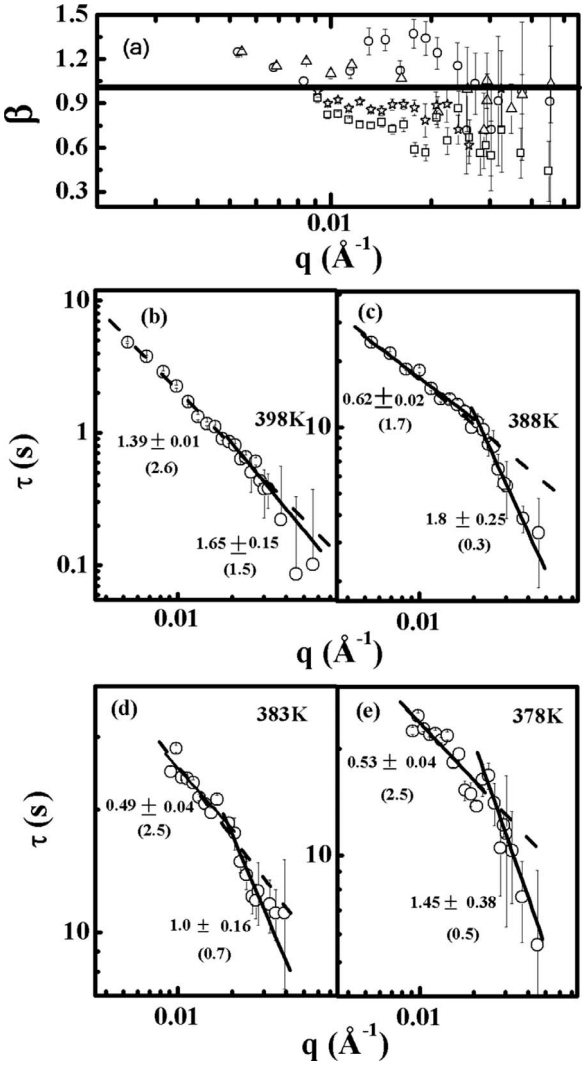

FIG. 7. (a) β vs q for sample with ϕ=0.012 at different measured temperatures (T), ○, 398 K; △, 388 K; ★, 383 K; □, 378 K. Relaxation time, τ vs q, at various measured temperatures. (b) T =398 K, (c) T=388 K, (d) T=383 K, and (e) T=378 K. The values of β and τ were extracted from fits to the $g_2(t)$ data using Eq. (2) and Eq. (3) in Eq. (1). Solid lines are the linear fits to the respective data in low and high wave-vector regions. Dashed lines are the fits to the same data over the entire measured range of wave vector. Indicated alongside each fitted curve is the estimate of respective α (α_l, α_h) obtained from the analysis using Eq. (3). The numbers within parentheses are the estimates of standard deviation for the obtained fits. The α value for the fit over the whole q range at 398 K, 388 K, 383 K, and 378 K is 1.39 ± 0.01 (1.87), 0.67 ± 0.01 (1.97), 0.58 ± 0.03 (1.97), and 0.54 ± 0.03 (2.05), respectively.

in a way qualitatively different. Even for the lowest measured temperature (378 K) we do not find any evidence of stretched exponential relaxation as was found for sample B. Although we do not have data for the lowest possible q for all temperatures it is clear from the 408 K data that β depends on q, decreasing from a value of ~1.4 at low q to ~1 at $q \sim 0.02$ Å^{-1} similar to what was predicted by Bouchaud *et al.* [23]. The dependence of τ on wave vector also changes significantly from that for samples A and B. As Figs. 8(b)–8(e) show, there does not seem to be any crossover in dynamics in terms of the wave-vector dependence of α, as was found for samples A and B. Also the α values seem to be almost independent of temperature. How can one understand such complex and puzzling behavior in these polymer nanocomposites as a function of temperature, volume fraction, and wave vector?

To obtain an insight into the dynamics of our PNC system we summarize the variation of exponent, α [defined in Eq. (3)] as a function of temperature for all volume fractions studied here and for $q < q_c$ (α_l) and $q > q_c$ (α_h), in Fig. 9. It is clear from Fig. 9(a) that α_l increases from a low-temperature value of $\alpha_l \leqslant 1$ to $\alpha_l > 1$ at high-temperature for samples A and B. Similarly, in Fig. 9(b) we show how α_h increases with temperature for samples A and B. In general $\alpha_h > \alpha_l$ at the same temperature and volume fraction. Further, $\alpha_h \to 2$ at high temperature for both low (sample A) and intermediate (sample B) volume fractions, there is indication of onset of pure diffusive behavior. However, for the highest

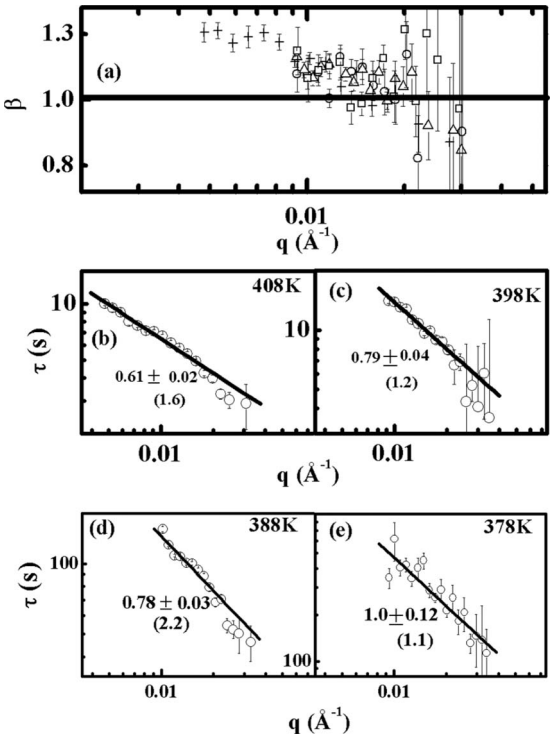

FIG. 8. (a) β vs q for sample with ϕ=0.077 at different measured temperatures, +, −408 K; ○, −398 K; △, 388 K; □, 378 K. Relaxation time, τ vs q at various measured temperatures. (b) T =408 K, (c) T=398 K, (d) T=388 K, and (e) T=378 K. The values of β and τ were extracted from fit to the $g_2(t)$ data Eq. (2) and Eq. (3) in Eq. (1). Solid lines are the fits to the same data over the entire measured range of wave vector. Indicated alongside each fitted curve is the estimate of respective α obtained from the analysis using Eq. (3). The numbers within parentheses are the estimates of the standard deviation for the obtained fits.

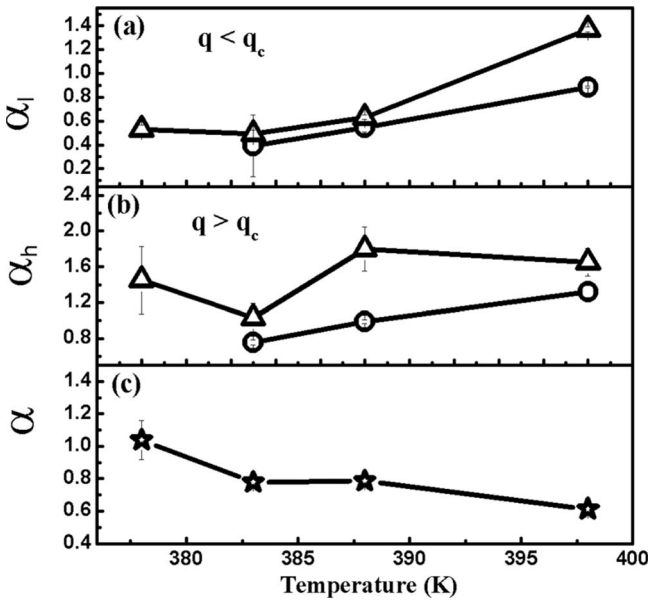

FIG. 9. α vs T, obtained from linear fits in Figs. 6–8 for different sample A (○), sample B (△), and sample C (★). (a) α_l, (b) α_h, and (c) α.

volume fraction (sample C) the exponent α is almost independent of wave vector, q and τ. The variation of α for this sample with temperature, T, is shown in Fig. 9(c). This wave-vector-dependent nonexponential relaxation indicates possible onset of a form of dynamic heterogeneity in the PNC systems. If we define $l_c \propto 1/q_c$ as a length scale corresponding to the crossover wave vector then this provides an estimate of the smallest region in the system where dynamics is spatially heterogeneous. It might be noted here that qualitatively similar behavior of length scale dependent relaxation was also observed in recent molecular dynamic simulation of colloidal gels and a similar length scale was identified where there is a crossover in the dynamics [25]. This crossover effect in dynamics seems to diminish at high T and ϕ and is most prominent for the sample with intermediate ϕ. It has been observed that [31,32] an intrinsic length scale for a supercooled liquid corresponding to onset of dynamic heterogeneity l_{CRR} exists below which diffusion is anomalous and $\alpha \rightarrow 0$, while above it normal diffusion with $\alpha \rightarrow 2$ exists. It is reasonable to assume that $l_{\mathrm{CRR}} \sim \xi_{\mathrm{CRR}}$, which for our PNC has been measured to be ~25 Å [4]. This corresponds to a q_{CRR} of ~0.3 Å^{-1} which is not reachable in a typical XPCS measurements. For our PNC system $\alpha < 2$ for $q > q_c$, especially at low q and low temperatures for the lowest volume fractions and at all temperatures for the highest ϕ. In fact for the highest ϕ, we have used for our measurements, this jamming effect increases to such an extent that the crossover in dynamics is not clearly observed within the measurable q range [Figs. 8(b)–8(e)]. It is not clear why this behavior is observed but could be indicative of particle-induced jamming, especially at higher volume fractions. It is of course possible that the expected diffusive behavior would be recovered if data could be collected at lower q.

Clearly our systems not only exhibit dynamics of some of the conventional phases found in other related soft and glassy systems but exhibits qualitatively different new types of dynamics, for certain values of T, ϕ or q which, to our knowledge, has not been found earlier. The realization of various applications of PNC utilizing their electrical, optical, and other physical properties which have been envisaged, will depend to a great extent as their thermomechanical properties. Use of polymer capped nanoparticles dispersed in homopolymer matrix has been found to be an effective strategy to overcome the problem of nanoparticle clustering in polymer nanocomposites which is deemed to be a major obstacle towards realization of the above applications. We had shown earlier [4] how for polymer capped nanoparticles dispersed in homopolymer matrix the glass transition is sensitive not only to the volume fraction of embedded nanoparticles but also to the interface morphology. Here we show how the microscopic dynamics is also sensitive to volume fraction of gold in PMMA matrix. Moreover, we also show that even PNC samples with similar magnitudes of T_g can have significantly different dynamics. It is well known that under certain conditions the intermediate scattering functions can be inverted to obtain time-dependent mean-squared deviation which can be further utilized for obtaining microrheological properties [33]. The difference in ISF for the PNC samples and especially between samples B and C having almost iden-

tical T_g and could thus be interpreted as due to the underlying difference in their respective microrheological properties.

IV. CONCLUSION

We have presented systematic studies of dynamics in a typical PNC system consisting of PMMA-capped gold nanoparticles embedded in PMMA matrix of identical molecular weight with various volume fractions. Our temperature and wave-vector-dependent XPCS measurements provides insight into the complex dynamics in these systems and reveals possible existence of a dynamical heterogeneity length scale intrinsic to PNC systems. The phase behavior in such systems is more complex and interesting and requires extensive investigation to fully understand the physics at the microscopic scale leading to such complex behavior. Our results also indicate why it is important to study various aspects of thermomechanical properties of various PNC systems to obtain an understanding of their processibility and possibly even mechanical integrity. In turn this information could determine their ultimate usefulness or otherwise in various possible applications exploiting their multifunctionality, as alluded to in the introduction.

ACKNOWLEDGMENTS

The authors acknowledge M. Sprung (APS) for discussions and A. Sandy (APS) for assistance in experiments. This work benefited by the use of facilities at APS, which is supported by U.S. DOE (BES) under Contract No. W-31-109-Eng-38 to the University of Chicago. Part of the work has been supported by DST, India and UCSD.

[1] R. B. Thompson, V. V. Ginzburg, M. W. Matsen, and A. C. Balazs, Science **292**, 2469 (2001).
[2] M. E. Mackay *et al.*, Science **311**, 1740 (2006).
[3] A. C. Balazs, T. Emrick, and T. P. Russell, Science **314**, 1107 (2006).
[4] S. Srivastava and J. K. Basu, Phys. Rev. Lett. **98**, 165701 (2007).
[5] L. Cipelletti and L. Ramos, J. Phys.: Condens. Matter **17**, R253 (2005).
[6] P. Sollich, F. Lequeux, P. Hebraud, and M. E. Cates, Phys. Rev. Lett. **78**, 2020 (1997).
[7] A. S. Keys, A. R. Abate, S. C. Glotzer, and D. J. Durian, Nat. Phys. **3**, 260 (2007).
[8] K. Statford, R. Adhikari, I. Pagonabarraga, J. C. Desplat, and M. E. Cates, Science **309**, 2198 (2005).
[9] B. Chung, S. Ramakrishnan, R. Bandyopadhyay, D. Liang, C. F. Zukosi, J. L. Harden, and R. L. Leheny, Phys. Rev. Lett. **96**, 228301 (2006).
[10] P. Chaudhuri, L. Berthier, and W. Kob, Phys. Rev. Lett. **99**, 060604 (2007).
[11] C. Caronna, Y. Chushkin, A. Madsen, and A. Cupane, Phys. Rev. Lett. **100**, 055702 (2008).
[12] A. Bansal *et al.*, Nature Mater. **4**, 693 (2005).
[13] P. Rittigstein, R. D. Priestley, L. J. Broadbelt, and J. M. Torkelson, Nature Mater. **6**, 278 (2007).
[14] R. Aravinda Narayanan, P. Thiyagarajan, S. Lewis, A. Bansal, L. S. Schadler, and L. B. Lurio, Phys. Rev. Lett. **97**, 075505 (2006).
[15] R. Krishnamoorti and R. A. Vaia, J. Polym. Sci., Part B: Polym. Phys. **45**, 3252 (2007).
[16] S. Sen, J. D. Thomin, S. K. Kumar, and P. Keblinski, Macromolecules **40**, 4059 (2007).
[17] S. E. Harton and S. K. Kumar, J. Polym. Sci., Part B: Polym. Phys. **46**, 351 (2008).
[18] J. B. Hooper and K. S. Schweizer, Macromolecules **40**, 6998 (2007).
[19] G. J. Papakonstantopoulos, M. Doxastakis, P. F. Nealey, J. L. Barrat, and J. J. de Pablo, Phys. Rev. E **75**, 031803 (2007).
[20] V. Pryamitsyn and V. Ganesan, Macromolecules **39**, 844 (2006).
[21] A. Bansal *et al.*, J. Polym. Sci., Part B: Polym. Phys. **44**, 2944 (2006).
[22] L. Cipelletti, S. Manley, R. C. Ball, and D. A. Weitz, Phys. Rev. Lett. **84**, 2275 (2000).
[23] J. P. Bouchaud and E. Pitard, Eur. Phys. J. E **6**, 231 (2001).
[24] V. Trappe, V. Prasad, L. Cipelletti, P. N. Segre, and D. A. Weitz, Nature (London) **411**, 772 (2001).
[25] E. Del Gado and W. Kob, Phys. Rev. Lett. **98**, 028303 (2007).
[26] P. I. Hurtado, L. Berthier, and W. Kob, Phys. Rev. Lett. **98**, 135503 (2007).
[27] A. Duri and L. Cipelletti, Europhys. Lett. **76**, 972 (2006).
[28] V. Trappe, E. Pitard, L. Ramos, A. Robert, H. Bissig, and L. Cipelletti, Phys. Rev. E **76**, 051404 (2007).
[29] H. Kim, A. Ruhm, L. B. Lurio, J. K. Basu, J. Lal, D. Lumma, S. G. J. Mochrie, and S. K. Sinha, Phys. Rev. Lett. **90**, 068302 (2003).
[30] R. Metzler and J. Klafter, Phys. Rep. **339**, 1 (2000).
[31] D. A. Stariolo and G. Fabricius, J. Chem. Phys. **125**, 064505 (2006).
[32] L. Berthier, D. Chandler, and J. P. Garrahan, Europhys. Lett. **69**, 320 (2005).
[33] A. Papagiannopoulos, T. A. Waigh, A. Fluerasu, C. Fernyhough, and A. Madsen, J. Phys.: Condens. Matter **17**, L279 (2005).